

## Tumorigenesis and Neoplastic Progression

# Down-Regulation of *WAVE3*, a Metastasis Promoter Gene, Inhibits Invasion and Metastasis of Breast Cancer Cells

Khalid Sossey-Alaoui,\* Alfiya Safina,\* Xiurong Li,\*  
Mary M. Vaughan,† David G. Hicks,†  
Andrei V. Bakin,\* and John K. Cowell\*

From the Departments of Cancer Genetics\* and Pathology,†  
Roswell Park Cancer Institute, Buffalo, New York

**The expression of *WAVE3*, an actin-cytoskeleton and reorganization protein, is elevated in malignant human breast cancer, yet the role of *WAVE3* in promoting tumor progression remains undefined. We have recently shown that knockdown of *WAVE3* expression in human breast adenocarcinoma MDA-MB-231 cells using small interfering RNA resulted in a significant reduction of cell motility, migration, and invasion, which correlated with a reduction in the levels of active p38 mitogen-activated protein kinase. Here, we investigated the effect of stable suppression of *WAVE3* by short hairpin RNA on tumor growth and metastasis in xenograft models. Breast cancer MDA-MB-231 cells expressing short hairpin RNA to *WAVE3* (sh*WAVE3*) showed a significant reduction in Matrigel invasion and formation of lung colonies after tail-vein injection in SCID mice. In the orthotopic model, we observed a reduction in growth rate of the primary tumors, as well as in the metastases to the lungs. We also show that suppression of p38 mitogen-activated protein kinase activity by dominant-negative p38 results in comparable phenotypes to the knockdown of *WAVE3*. These studies provide direct evidence that the *WAVE3*-p38 pathway contributes to breast cancer progression and metastasis. (*Am J Pathol* 2007, 170:2112–2121; DOI: 10.2353/ajpath.2007.060975)**

The processes of cellular migration and invasion are critical for the ability of tumor cells to metastasize locally and to distant sites.<sup>1</sup> These events are controlled by a complex interaction of genetic pathways that can be specific to different cell types and facilitated through disruption of phenotypes that restrict the motility of the cell type involved.<sup>2</sup> These phenotypic changes occur on a background of genetic events that allow the cell to

invade surrounding tissue as well as access the vasculature to facilitate relocation to distant organs. This latter process can only be achieved if the metastasizing cell can survive in the blood stream and re-establish in the new organ site. Although the matrix metalloproteinases are perhaps the best studied proteins facilitating tumor cell invasion, the factors regulating the actin cytoskeleton dynamics have recently emerged as critical contributors to the metastatic phenotype.<sup>2–6</sup>

Cell motility and invasion require highly coordinated regulation of actin dynamics within the cell.<sup>7,8</sup> The proteins that influence this process have been implicated in metastasis.<sup>3–6,9,10</sup> We have recently shown that *WAVE3*, a member of a WASP protein family controlling actin polymerization, has a profound effect on motility and invasion of breast cancer cells. The proteins of this family regulate actin polymerization through the recruitment of the Arp2/3 protein complex via a verprolin-cofilin-acidic domain at the C terminus. It is thought that the formation of the multimeric complex comprising the verprolin-cofilin-acidic domain, the actin monomer, and the Arp2/3 complex is a critical step in actin polymerization.<sup>11,12</sup> We have found that suppression of *WAVE3* by small interfering RNA (siRNA) in breast cancer MDA-MB-231 cells dramatically reduces lamellipodia at the migrating edge while increasing actin stress fibers linked to focal adhesion, which are generally associated with static cells.<sup>9,10</sup> This *in vitro* phenotype was accompanied by a significant decrease of cell migration and invasion, suggesting that *WAVE3* is a critical factor that regulates the

---

Supported in part by the American Cancer Society (institutional research grant IRG02-197-01 to K.S.A.), the Public Health Service (grant R01 CA95263 to A.V.B.), the United States Army Medical Research and Materiel Command (grant DAMD17-02-01-0602 to A.V.B.), the National Institutes of Health (grant NS35791-05 to J.K.C.), and the National Cancer Institute–Roswell Park Cancer Institute Cancer Center Support grant CA 16056.

Accepted for publication February 27, 2007.

Address reprint requests to Khalid Sossey-Alaoui, Ph.D., Roswell Park Cancer Institute, Department of Cancer Genetics, Elm and Carlton Sts., Buffalo, NY 14263. E-mail: khalid.sossey-alaoui@roswellpark.org.

motility and adhesiveness of cells.<sup>9,10</sup> Our studies also indicate that p38 mitogen-activated protein kinase (MAPK) and matrix metalloproteinases are downstream effectors of WAVE3 in cell motility and invasion.<sup>10</sup>

Here, we investigated whether disruption of WAVE3 and/or p38MAPK function affects the malignant phenotype of breast cancer MDA-MB-231 cells using mouse xenograft models. WAVE3 was suppressed by stable expression of siRNA, whereas p38MAPK signaling was blocked by expression of a dominant-negative p38  $\alpha$  (p38AGF). Disruption of either WAVE3 or p38 reduced formation of tumors on the lung surface indicating that WAVE3-p38 MAPK signaling contributes to the metastatic potential of breast cancer cells. Importantly, the immunohistochemical analysis of breast cancer samples showed that WAVE3 protein levels correlate with tumor grade. Together these findings provide evidence that WAVE3 is an important factor in breast cancer progression by contributing to tumor cell motility and invasion.

## Materials and Methods

### Materials

SuperScript II reverse transcriptase kits and *Taq* polymerase were obtained from Invitrogen (Carlsbad, CA). Polymerase chain reaction (PCR) primers were synthesized by Integrated DNA Technologies (Coralville, IA). The primer sequences used for GAPDH were 5'-GAAGG-GAAGGTCGGAGT-3' for the forward primer and 5'-GAA-GATGGTGTATGGGATTT-3' for the reverse primers. Primers for WAVE3 were as previously reported.<sup>13</sup> The antibodies used in this study were as follows: rabbit anti-human WAVE3/Scar antibodies from either Upstate Biotechnology (Charlottesville, VA) or from New England Peptide, Inc. (Gardner, MA); mouse anti-human PI3-kinase p85 obtained from BD Biosciences (San Diego, CA), and rabbit anti-human vascular endothelial growth factor (VEGF) from Santa Cruz Biotechnology (Santa Cruz, CA). Secondary antibodies were obtained from Amersham Biosciences (GE Healthcare, Buckinghamshire, UK).

### Animals

Eight-week-old female SCID/CB17 mice were obtained from the Department of Laboratory Animal Resources facility colony at the Roswell Park Cancer Institute. All animals were kept three to five mice per cage in microisolator units and provided with water and food according to a protocol approved by the Institute Animal Care and Use Committee at Roswell Park Cancer Institute. The facility is certified by the American Association for Accreditation of Laboratory Animal Care and is in accordance with current regulation and standards of the US Department of Agriculture and the US Department of Health and Human Services.

### Retrovirus Production

A retroviral vector containing a short hairpin RNA against WAVE3 (catalog no. RHS1764-9702604) was obtained from Open Biosystems (Huntsville, AL). Plasmid DNA was purified from *Escherichia coli* cells using the Invitrogen mini prep kit. A stock of the retrovirus was prepared using PT67 packaging cells and the CalPhos mammalian transfection kit (BD Biosciences, Palo Alto, CA), following the manufacturer's instructions. PT67 clones producing shWAVE3 retroviruses were selected 24 hours after transfection using puromycin. The puromycin-resistant clones were isolated by ring cloning and propagated in puromycin-containing culture media. Conditioned medium containing the packaged virus was collected every other day. Cell debris were removed by centrifugation of the conditioned medium for 5 minutes at 2000 rpm, and virus particles were filter-purified using 0.45- $\mu$ m syringe filters with low protein binding (Pall Corp., Ann Arbor, MI). MDA-MB-231 cells were infected in a six-well plate. Individual puromycin-resistant clones were selected by ring-cloning and propagated in puromycin-containing media. WAVE3 knockdown in these clones was confirmed by reverse transcriptase (RT)-PCR and Western blot analyses.

### Cell Culture and Transfections

The human breast cancer MDA-MB-231 cells were obtained from American Type Culture Collection (Rockville, MD). MDA-MB-231 expressing dominant-negative p38alpha has recently been described.<sup>14</sup> Cells were cultured at 37°C with 10% CO<sub>2</sub> in Dulbecco's modified Eagle's medium (DMEM) supplemented with 4.5 g/L glucose, 10% fetal bovine serum (Invitrogen), 2 mmol/L glutamine, and antibiotics. For transient transfections,  $\sim 2.5 \times 10^5$  cells were plated in either 60-mm dishes or six-well plates in DMEM without antibiotics 24 hours before transfection. Transfections were performed using Oligofectamine (Invitrogen) in OPTI-MEM (Invitrogen) media as directed by the manufacturer. Approximately 4 to 12 hours after transfection, medium was supplemented with DMEM containing 10% fetal bovine serum without antibiotics.

### Reverse Transcription-PCR

Cells were lysed in TRIzol reagent (Invitrogen), and total RNA was extracted according to the manufacturer's instructions. RNA was quantified using a spectrophotometer (Beckman-Coulter, Fullerton, CA), and 1  $\mu$ g of RNA was used to generate cDNA with the SuperScript II RT-PCR kit (Invitrogen). Reverse transcription was performed according to the manufacturer's instructions, and the cDNA generated was used as a template for 30 cycles of PCR amplification for analysis of gene expression using a PTC-100 thermal cycler from MJ Research (Waltham, MA).

### *Immunoblot Analysis*

Whole cell lysates containing equivalent amounts of total protein (50  $\mu\text{g}$ ) were resolved on a 10% sodium dodecyl sulfate-polyacrylamide gel, followed by transfer to nitrocellulose (Bio-Rad, Hercules, CA) or Immobilon-P (Millipore, Billerica, MA) membranes using the Bio-Rad gel and transfer apparatus. Membranes were incubated in 5% whole milk (or bovine serum albumin) for 1 hour at room temperature, washed with phosphate-buffered saline (PBS), followed by incubation with the primary antibody (as specified) overnight at 4°C. Membranes were then washed and incubated in the appropriate secondary antibody at room temperature for 1 hour, and the immunocomplexes were visualized using the Western Lights chemiluminescence detection kit from Perkin-Elmer (Boston, MA).

### *Matrigel Invasion Assay*

The invasive potential of parental MDA-MB-231 cells and the WAVE3 knockdown cells was assessed using the Matrigel invasion chambers from BD Biosciences (San Diego, CA). Cells were cultured for 48 hours in complete media, harvested by trypsinization, and counted, and  $5 \times 10^4$  cells were placed onto the top insert. One chamber consists of a cell insert and a well. The bottom of the cell insert is covered with a filter containing multiple 8- $\mu\text{m}$  pores and is coated with a basement membrane matrix (Matrigel). Cells, in 500  $\mu\text{l}$  of serum-free DMEM media, were seeded in the cell insert and placed in the well, which was filled with 750  $\mu\text{l}$  of DMEM and supplemented with 10% fetal bovine serum. After 24 hours of incubation at 37°C and 5%  $\text{CO}_2$ , the noninvasive cells present on the upper surface of the filter were removed using a sterile cotton swab. The cells that were able to migrate through the Matrigel onto the lower surface of the filter were fixed and stained with Diff-Quick (American Scientific Products, McGraw Park, IL). The lower surface of the filter was photographed using an inverted Leica DM IRB microscope fitted with a charge-coupled device camera (Leica Microsystems, Wetzlar, Germany), and migrating cells were counted from four fields at  $\times 200$  magnification.

### *Spontaneous Metastasis Model*

In this model, also referred to as orthotopic xenograft model, exponentially growing cells ( $1 \times 10^6$ ) in 0.1 ml of Hanks' buffered salt solution were inoculated into the surgically exposed mammary fat pad of 6- to 8-week-old female SCID mice. At this age, the mammary glands are fully developed. Injected tumor cells grow locally and eventually metastasize to other sites. The growth of primary tumors was monitored twice a week by measuring tumor diameters with calipers and calculating tumor volume using the formula: volume = width<sup>2</sup>  $\times$  length/2. Tumor take by MDA-MB-231 cells in SCID mice is typically 100%. Primary tumors were removed at 1 cm in diameter (typically, 30 to 35 days after inoculation). The tumors were excised and either frozen in liquid  $\text{N}_2$  or

formalin-fixed. The mice were sacrificed 4 to 5 weeks later, and their lungs, spleen, and livers were collected for histological analysis for metastases. Tumors that were recovered from the primary sites as well as from the metastatic sites were assayed for continued knockdown of WAVE3 expression using both RT-PCR and Western blot. Sectioning and hematoxylin and eosin (H&E) staining were performed by the pathology core facility at Roswell Park Cancer Institute. Primary tumors were evaluated by light microscopy and immunohistochemistry for expression of WAVE3.

### *Experimental Metastasis Model*

In the experimental metastasis model, tumor cells ( $2 \times 10^6$ ) resuspended in 0.15 ml of sterile Hanks' solution were injected using a 28-gauge needle into a tail vein of 6- to 8-week-old female SCID mice. Mice were sacrificed 4 weeks later. Lungs were stained with 15% black Indian ink using a 19-gauge needle and a 5-ml syringe, administered through the trachea as described previously.<sup>14</sup> Tumor cells do not take up the ink and appear as white spots on the lung. The lungs were then dissected from the thoracic cage with scissors and placed in Fekete's solution for 24 hours. Lung surface macrometastatic lesions, which appear as white spots, were counted and a comparison made between cells expressing WAVE3 and those that do not.

### *Histopathological Analyses*

The breast cancer specimens obtained from the Roswell Park Cancer Institute breast repository were reviewed and graded by a single pathologist (D.G.H.), using the standard Scarff-Bloom-Richardson grading system. Dr. Hicks also determined the progesterone receptor and the estrogen receptor status using immunohistochemistry and the DAKO scoring system (DAKO, Carpinteria, CA).

### *Immunohistochemistry*

Tumors and tissues were recovered by surgery and embedded in paraffin by routine diagnostic procedures. Paraffin sections (5  $\mu\text{m}$ ) were cut at 5  $\mu\text{m}$ , placed on charged slides, and dried in a 60°C oven for 1 hour. Room temperature slides were deparaffinized in three changes of xylene and rehydrated using graded alcohols. Endogenous peroxidase was quenched with aqueous 3%  $\text{H}_2\text{O}_2$  for 10 minutes and washed with PBS/T. Antigen retrieval was then done with citrate buffer, pH 6, in the microwave for 10 minutes and allowed to cool for 15 minutes followed by a PBS/T wash. The slides were then placed on the DAKO autostainer, and the following program was run: PBS/T wash followed by a 30-minute incubation in 0.03% casein in PBS/T, and a 1-hour incubation at room temperature with 0.5  $\mu\text{g}/\text{ml}$  rabbit anti-WAVE3 (New England Peptide, Inc.). Rabbit IgG at 0.5  $\mu\text{g}/\text{ml}$  was used on a duplicate slide in place of the primary antibody as a negative control. A PBS/T wash was followed by biotinylated secondary goat anti-rabbit

antibody for 30 minutes. A PBS/T wash was followed by the ABC reagent (Vector Laboratories, Burlingame, CA) for 30 minutes. Slides were washed in PBS/T and the chromogen diaminobenzidine (DAKO) was applied for 5 minutes (color reaction product, brown). The slides were then counterstained with hematoxylin, dehydrated, cleared, and coverslipped.

### Statistical Analysis

Tumor volume, body weights, number of invading cells, and number of lung metastases were represented as mean  $\pm$  SE. The Student's *t*-test was used for the statistical analysis. A *P* value of  $<0.05$  was considered significant.

## Results

### Down-Regulation of WAVE3 with Short Hairpin RNAs Reduces Invasiveness of MDA-MB-231 Cells

We have previously shown that transient transfection of siRNA oligonucleotides to *WAVE3* effectively reduces *WAVE3* protein levels.<sup>9,10</sup> Because the knockdown effect only lasts  $\sim 5$  days, it was not possible to undertake *in vivo* studies that require prolonged suppression of the target protein. To overcome this limitation, we generated a series of MDA-MB-231-derived clones that stably express short hairpin RNAs (shRNAs) against *WAVE3* (Figure 1). Immunoblot analysis showed that protein levels of *WAVE3* were reduced greater than 90% in all but one (no. 15) clone (Figure 1A). *WAVE3* knockdown in these clones was also confirmed at the mRNA level using RT-PCR analysis (Figure 1B). Reanalysis of these clones throughout a 9-month period showed that the reduction of *WAVE3* levels was sustained. In addition, we have previously shown that transient suppression of *WAVE3* using siRNA reduces motility and invasiveness of MDA-MB-231 cells.<sup>10</sup> We also showed that this reduction in motility and invasiveness is a direct result of loss of *WAVE3* expression, because the mock siRNA did not have any effect on *WAVE3* expression levels, cell motility, or cell invasion.<sup>10</sup> Thus, in all of the experiments described below, only the parental MDA-MB-231 cells were used for the control experiments. Next, we evaluated the effects of stable knockdown of *WAVE3* in the 231-derivative clones on *in vitro* invasion using the Matrigel assay. In all five clones analyzed, a fourfold to fivefold reduction in the number of cells invading the Matrigel-covered membrane was seen, compared with the control cells (Figure 1C), clearly demonstrating that suppression of *WAVE3* levels using shRNA effectively reduces the invasive capability of MDA-MB-231 cells *in vitro*. These results are also entirely consistent with our studies using transient transfections of siRNAs to *WAVE3*.<sup>10</sup>

### WAVE3 Is Highly Expressed in Advanced Stages of Breast Cancer

Our previous studies revealed high levels of *WAVE3* expression in the majority of metastatic breast cancer cell lines,<sup>9,10</sup>

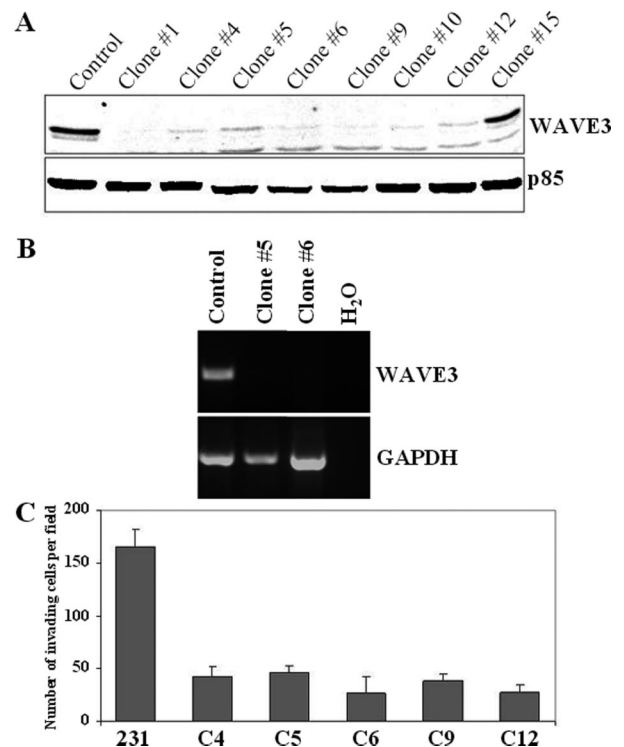


**Figure 1.** Knockdown of *WAVE3* expression with shRNA inhibits *in vitro* invasion of MDA-MB-231 cells. **A:** Western blot analysis of *WAVE3* protein in independent clones derived from MDA-MB-231 cells with stable expression of shRNAs against *WAVE3*. *WAVE3* protein levels were reduced to almost undetectable levels in all but clone 15. p85 protein was used as a loading control. **B:** RT-PCR analysis of *WAVE3* mRNA in clones 5 and 6. *WAVE3* mRNA expression was reduced to undetectable levels in clones 5 and 6. **C:** Results from the *in vitro* invasion assay shows the reduced ability of cells from independent clones with *WAVE3* down-regulation to migrate through the Matrigel membrane. There was an average of fivefold reduction in invasion ability compared with the parental cells.

suggesting that these elevated levels might be associated with the progression of breast cancer. Here, we analyzed *WAVE3* in breast tumor specimens from different breast cancer stages/grades using immunohistochemistry with polyclonal antibodies to *WAVE3*. The analysis showed that approximately threefold higher levels of *WAVE3* were present in grade III tumors compared with grade I tumors (Figure 2), whereas little or no *WAVE3* protein was detected in either the normal breast or grade I tumors. Interestingly, this analysis, with a *P* value approaching significance ( $P = 0.07$ ), also revealed an inverse correlation between the estrogen receptor/progesterone receptor status and *WAVE3* levels. Clearly, a much larger sample would be required to unambiguously confirm this observation. The biological significance of this correlation, however, remains to be determined. These findings indicate that *WAVE3* expression correlates with breast cancer progression.

### Down-Regulation of WAVE3 Inhibits Lung Metastasis of MDA-MB-231 Cells in SCID Mice

In the experimental metastasis model, when tumor cells are injected into the tail veins of immunocompromised mice, MDA-MB-231 cells are able to form tumors in the lungs and other organs.<sup>15,16</sup> Because the formation of



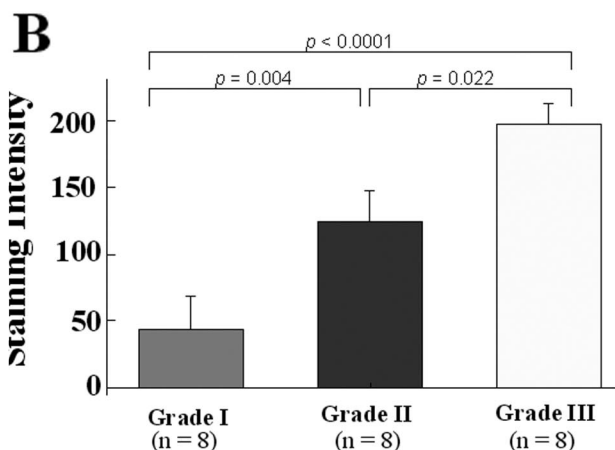
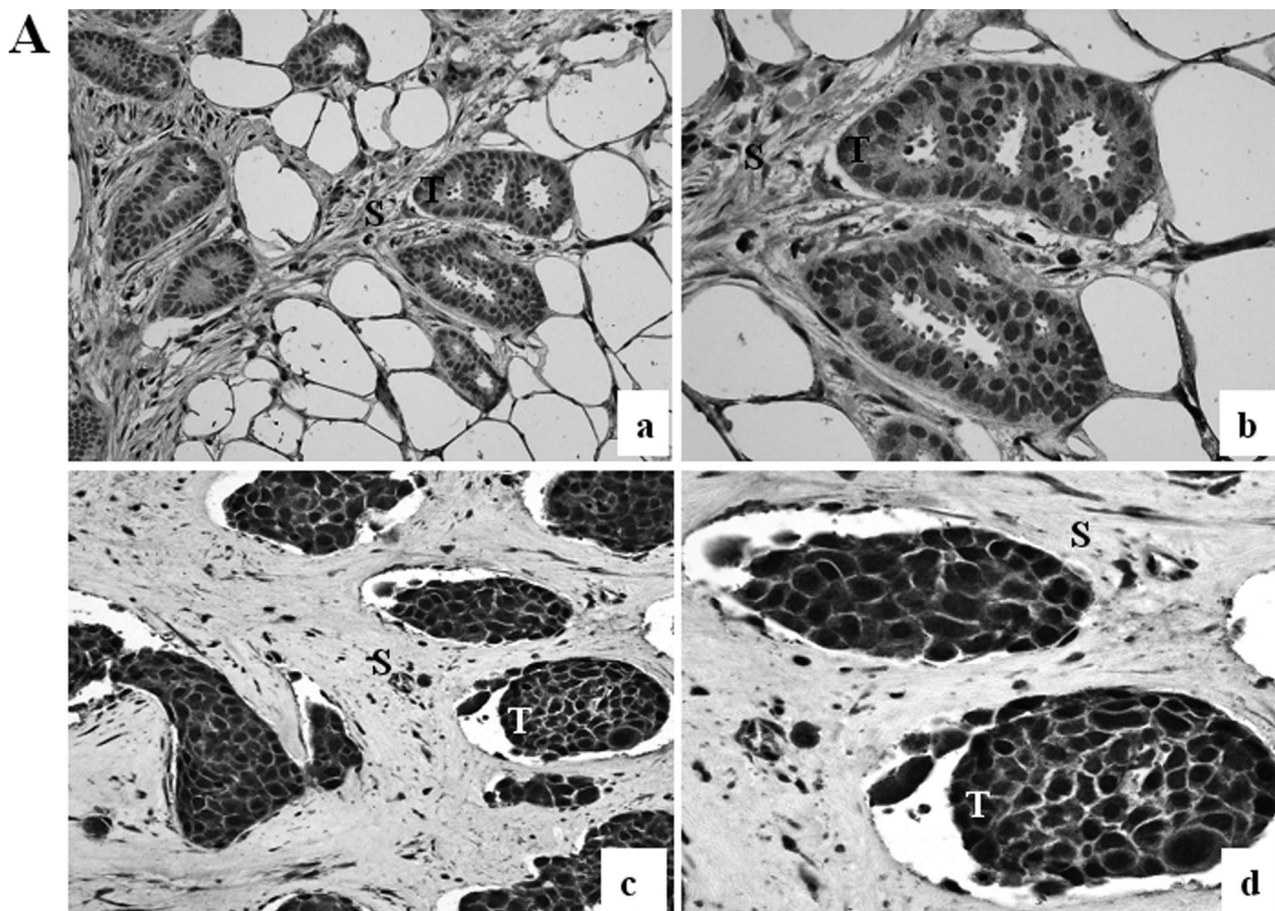


**Figure 2.** WAVE3 is overexpressed in human breast cancer. Immunohistochemical analysis of primary human breast cancer. In **A**, the top two panels (**a**, **b**) are from low-grade breast cancer showing weak staining for WAVE3 in the infiltrating tumor cells. The bottom two panels (**c**, **d**) are from a high-grade breast cancer showing a strong diffuse granular cytoplasmic pattern of staining in the infiltrating tumor cells. T, tumor; S, stromal tissue. WAVE3 staining in the tumors was scored as 0 for negative, 1 for weak, 2 for moderate, and 3 for strong. **B**: Comparison of the WAVE3 staining in the tissue sections demonstrates a significant difference between low- and high-grade tumors. The overall WAVE3 staining intensity was determined as the product of the percentage of positive cells and the staining score. Original magnifications:  $\times 200$  (**a**, **c**);  $\times 400$  (**b**, **d**).

metastases in this model depends on invasiveness, we first used this model to examine the effect of WAVE3 knockdown on the metastatic potential of MDA-MB-231 cells. Control MDA-MB-231 cells formed a significantly higher number of lung surface metastases after injection in the tail veins of SCID mice, compared with the WAVE3 knockdown cells (Figure 3, A and B). Although this model is typically used to measure tumor colonies on the lung surfaces, we also surveyed MDA-MB-231 metastasis to other organs using genomic DNA-based PCR with primers specific to the human *ERV6* DNA sequence. As

expected, a strong PCR product was detected in the lungs from the mouse injected with the parental cells (Figure 3C). Human-specific PCR products were also detected in the liver and, to a lesser extent, in the spleen from this group of mice (data not shown), which demonstrates that the MDA-MB-231 cells were able to reach these organs. The intensity of the human-specific PCR products in the lungs from the mouse injected with the shWAVE3 cells were quantified by densitometry. From five independent experiments, the ratio of the mean intensity values between the two groups showed an  $8.02 \pm$

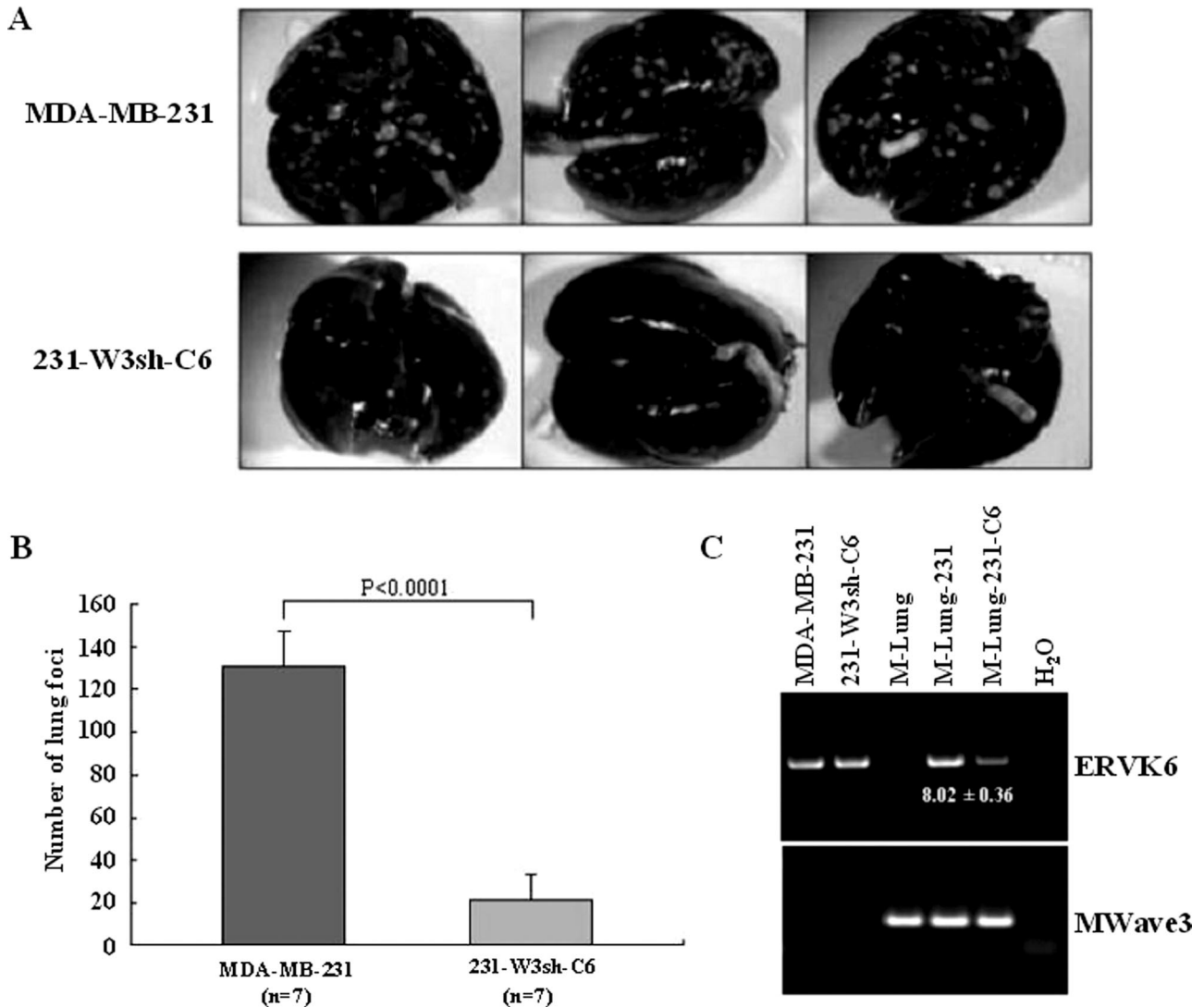


**Figure 3.** Knockdown of *WAVE3* expression inhibits *in vivo* metastasis in SCID mice. **A:** Pulmonary metastasis of MDA-MB-231 cells is suppressed by shRNA to *WAVE3*. A representative appearance of murine lungs with metastasized colonies (visible as white spots) from parental MDA-MB-231 cells, compared with the *WAVE3*-suppressed cells (clone 6 as an example), 5 weeks after intravenous injection. **B:** When the incidence of tumors on the surfaces of the lungs were counted in seven mice, the *WAVE3*-suppressed cells showed a significant decrease. **C:** PCR analysis of DNA from murine lungs after tail vein injection of shW3 clone 6 cells. The human-specific *ERVK6A* gene can be identified in human DNA (MDA-MB-231 and 231-shW3-C6) but not in mouse DNA (M-Lung). The presence of the human retroviral sequences in the mouse tissues (M-Lung-231 and M-Lung-231-C6) indicates the presence of human cells in these tissues. *ERVK6A* PCR amplification in M-Lung-231 relative to 231-shW3-C6 was calculated from the ratio of respective band intensities shown on the gel (fold  $\pm$  SD from five independent PCR reactions). The mouse *Wave3* gene is used as a control for integrity of the mouse DNA in each sample.

0.36-fold increase in the parental cells compared with the shWAVE3 cells (Figure 3C). This is consistent with a reduced number of lung-surface metastases in this group. However, no PCR products were found from the liver and spleen samples of the mice injected with the shWAVE3 cells (data not shown), indicating that loss of *WAVE3* in MDA-MB-231 cells prevented tumor cells from locating to these organs. Metastasis to the lungs was also surveyed by H&E staining of lung sections. Although the parental MDA-MB-231 cells produced large and numerous tumors, smaller and less frequent tumors were detected in the lungs of mice injected with the shWAVE3 cells (Figure 4), which parallels the number of metastases detected on the lung surfaces (Figure 3, A and B).

### *Suppression of WAVE3 Attenuates the Establishment of Primary Tumors of MDA-MB-231 Cells in SCID Mice*

MDA-MB-231 cells implanted into the mammary fat pads of female SCID mice rapidly form tumors at the site of injection.<sup>16</sup> This orthotopic xenograft model was used to measure tumor development, growth, and spontaneous metastasis of MDA-MB-231 cells with suppressed expression of *WAVE3*. These experiments were performed using clones C5 and C6 of MDA-MB-231 cells expressing shWAVE3. Tumors developed in all of the mice that were implanted with the control MDA-MB-231 cells (100% in-



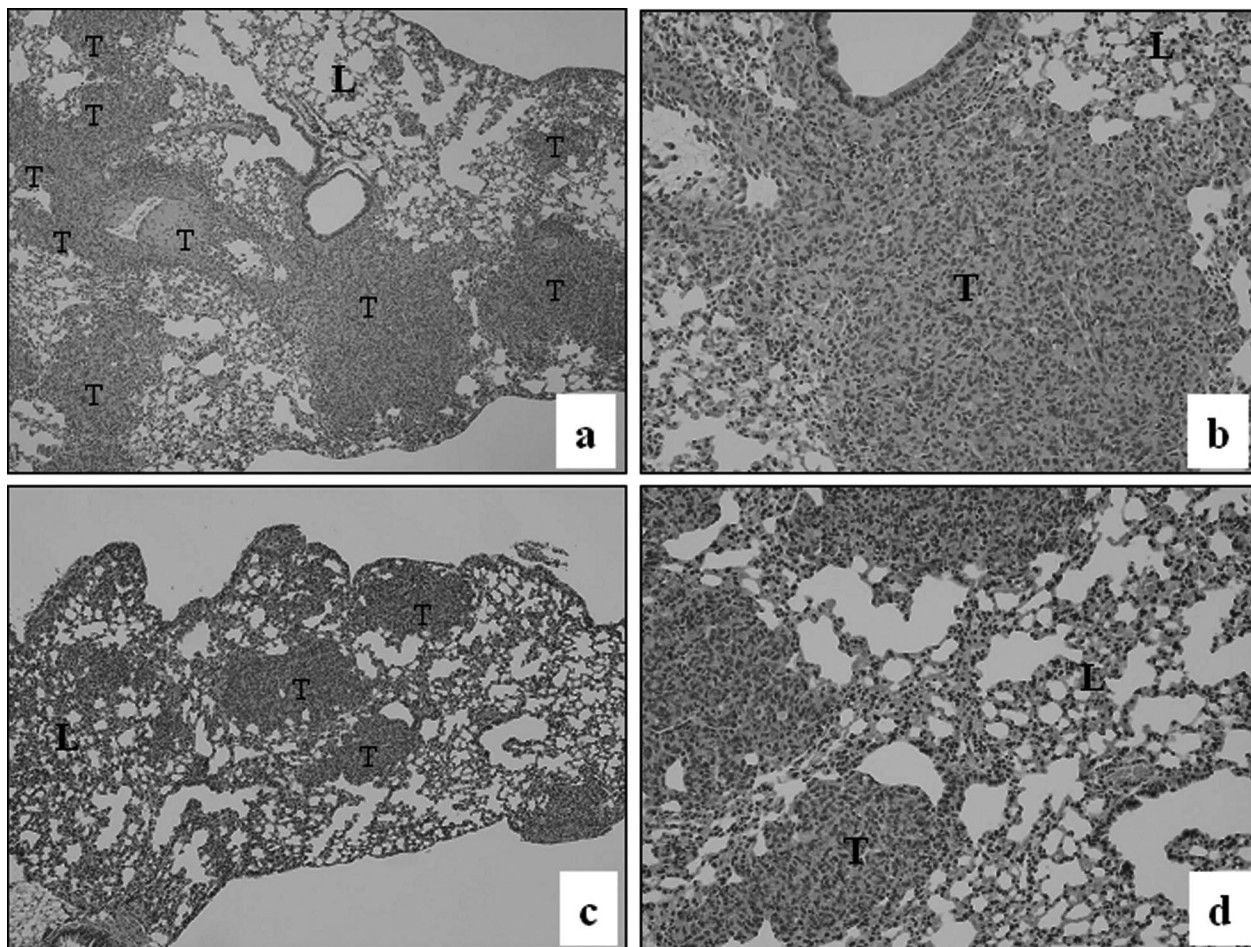


**Figure 4.** H&E staining of sections from lungs of mice injected with parental MDA-MB-231 cells (top) shows the presence of large tumors (**a, b**) compared with (bottom) lung metastases from the mice injected with cells expressing shWAVE3 (**c, d**). T, tumors; L, lung. Original magnifications:  $\times 40$  (**a, c**);  $\times 100$  (**b, d**).

cidence) within 22 days. In contrast, the tumor take was only 25% (two of eight mice) for the group of mice implanted with clone C5, and 50% (four of eight) for the group of mice implanted with clone C6 (Figure 5A). Tumor latency was also affected by *WAVE3* knockdown. In the control group, palpable tumors were detected as early as 15 days after inoculation (Figure 5A), whereas, in the shWAVE3 groups, the tumors were first palpable after 22 days for clone C6 or 40 days for clone C5 (Figure 5A).

To determine the effect of *WAVE3* knockdown on tumor growth rate, tumor size was monitored every 4 days, until they were either 1 cm in diameter or reached a volume of  $\sim 0.5$  cm<sup>3</sup>. In the control group, tumor volume reached 0.5 cm<sup>3</sup> as early as 32 days after implantation (Figure 5B). The tumors were surgically removed at day 47 after implantation, as tumors reached the maximum burden defined in the protocol. The mice were maintained for an additional 5 weeks before they were sacrificed and metastases to other organs analyzed. In contrast, tumor growth rate in the shWAVE3 cohorts was reduced by 40 and 80% for clones C6 and C5, respectively (Figure 5B). Even after 69 days after implantation, none of the tumors had reached 0.5 cm<sup>3</sup>, at which point all mice were sacrificed.

The analysis of spontaneous metastases in the orthotopic xenograft model showed that *WAVE3* knockdown

significantly reduced ( $P < 0.00001$ ) metastasis to the lungs (Figure 5C) compared with the control cells. Immunohistochemical analysis of the tumors derived from the *WAVE3* knockdown showed that the tumor cells retained low levels of *WAVE3* expression compared with those derived from the control cells (Figure 6A). Thus, knockdown of *WAVE3* not only reduces the rate of tumor growth at the primary site *in vivo* but also inhibits the formation of metastases in distant organs. This reduction in the growth rate is not a result of an inhibition of tumor cell proliferation because we have previously shown that knockdown of *WAVE3* expression had no effect on growth rate.<sup>17</sup>

Because tumor angiogenesis is critical for the establishment and development of tumors at both primary and metastatic sites, we determined whether *WAVE3* knockdown affects either tumor vasculature or the expression of *VEGF*. Staining with an anti-VEGF antibody revealed decreased levels of VEGF in the shWAVE3-derived tumors (Figure 6C), suggesting an association between the expression levels of VEGF and tumor vasculature. Immunohistochemical analysis using the antibody to CD31, a blood vessel-specific marker, demonstrated a substantial reduction in the number and size of blood vessels in the shWAVE3 tumors, compared with the tumors derived from the control cells (Figure 6, D and E).

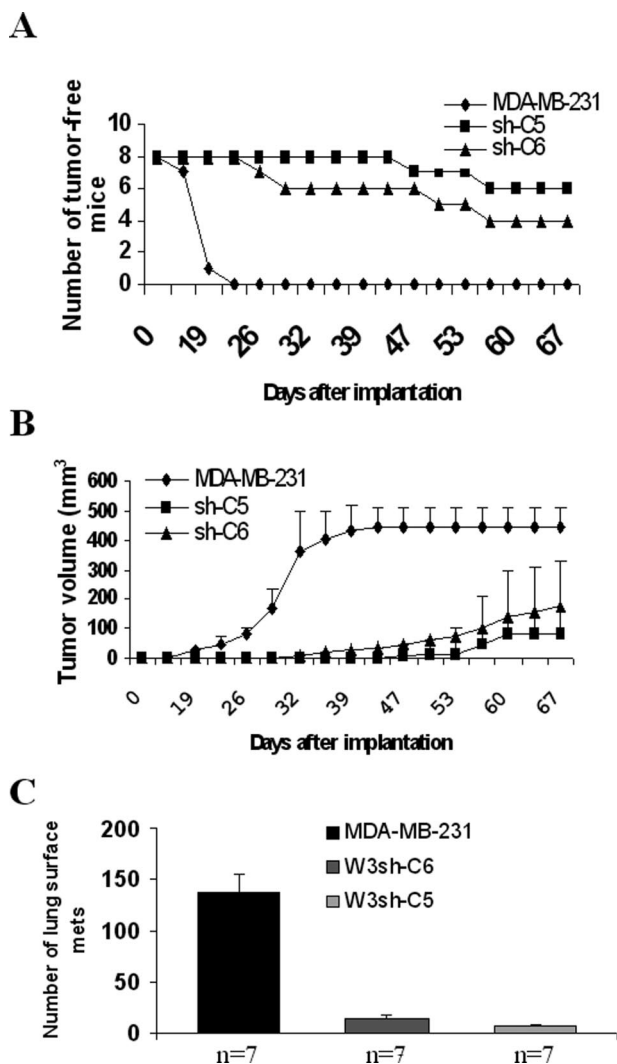


**Figure 5.** Effect of *WAVE3* knockdown on MDA-MB-231 tumor growth and lung metastasis in the spontaneous metastasis model. Tumor incidence and latency in mammary fat pads are shown in **A**, in which 100% of mice in the control group produced tumors, whereas the tumor incidence was reduced to 25 and 50% in the groups of mice implanted with clones W3sh-C5 and W3sh-C6, respectively. In **B**, the tumor growth curves represent the parental MDA-MB-231 cells, or C5 or C6, two clones derived from MDA-MB-231 cells expressing the shRNA against *WAVE3*, respectively. Each data point represents the mean of tumor volume  $\pm$  SD, showing a significant difference ( $P < 0.00001$ ) between the parental cells and the sh*WAVE3*-derived cells. Mice were monitored for 67 days after implantation, after which they were all sacrificed and analyzed for lung metastases. **C**: Pulmonary metastasis is also suppressed by *WAVE3* shRNA. The average number of lung metastases was  $\sim$ 10 times higher in the control group compared with the sh*WAVE3* groups ( $P < 0.00001$ ). *n*, number of mice per group.

### Blockade of p38MAPK Signaling Has Comparable Effects on Tumor Invasion to *WAVE3* Knockdown

Our previous studies have indicated that p38 mitogen-activated protein kinase (p38MAPK) is a downstream target of *WAVE3*.<sup>10</sup> Transient transfection of siRNA to *WAVE3* in MDA-MB-231 cells significantly reduces the levels of active p38MAPK.<sup>10</sup> To investigate whether inhibition of p38MAPK signaling also affects the metastatic potential of tumor cells, we used MDA-MB-231 cells ex-

pressing a dominant-negative mutant of *p38alpha* (DN-p38).<sup>14</sup> Compared with the cells expressing the control EGFP vector, expression of DN-p38 blocked phosphorylation of HSP27, a known downstream target of p38MAPK, but did not affect the p38 levels (Figure 7A). No significant changes were detected in the activity levels of ERK1/2 (Figure 7A). After injection in the tail veins of female SCID mice, cells expressing DN-p38 formed threefold fewer colonies on the lung surfaces, compared with the control EGFP-expressing cells (Figure 7B). This effect of DN-p38 (threefold reduction) was comparable with the effect of sh*WAVE3* (sixfold reduction), suggesting that p38MAPK is an important effector of *WAVE3* for the metastatic phenotype of tumor cells.

### Discussion

The present study provides evidence that *WAVE3* may play an important role in the acquisition of the metastatic potential of tumor cells. Based on the immunohistochemical analysis, *WAVE3* protein levels in breast cancer samples revealed a correlation between *WAVE3* levels and breast cancer progression. High-grade breast tumors exhibited elevated levels of *WAVE3* protein compared with normal breast epithelium and low-grade breast tumors. Suppression of *WAVE3* in MDA-MB-231 breast cancer cells significantly reduces the ability of tumor cells to form metastases in orthotopic and tail-vein xenograft models. Intriguingly, the *WAVE3* knockdown cells were less tumorigenic in SCID mice. These studies suggest that *WAVE3* may represent a marker of tumor progression and a potential target for anti-tumor therapy.

The WASP/*WAVE* proteins are key factors in the regulation of the actin cytoskeleton through activation of the Arp2/3 complex that initiates actin polymerization.<sup>11,12</sup> The activity of WASP/*WAVE* is regulated through the formation of hetero-complexes containing Sra1/PIR121, Nap1, Abi1/2, and HSPC300.<sup>18–20</sup> These complexes link small GTP-binding protein Rac, activated on stimulation with extracellular signals, to the *WAVE*-Arp2/3 complex to regulate the formation of different types of membrane ruffles, therefore regulating cell motility.<sup>21</sup> At least one member of the WASP/*WAVE* family, *WAVE2*, has been associated with the metastatic phenotypes of murine melanoma cells.<sup>17</sup>

Our study provides the first evidence for the role of *WAVE3* in tumor cell invasion and metastasis. In the experimental metastasis model, *WAVE3* was required for breast cancer cells to form tumor colonies in the lungs. This effect of *WAVE3* is apparently independent of the closely related *WAVE1* and *WAVE2* proteins, because their mRNA levels were not affected by siRNA to *WAVE3*.<sup>9,10</sup> Although the sh*WAVE3* cells were able to be established in the lungs, they form smaller sized colonies. The orthotopic xenograft studies showed that *WAVE3*-deficient cells were significantly less tumorigenic in SCID mice. Tumor incidence was reduced by 60 to 80% compared with control cells. Tumors that developed from the sh*WAVE3* cells grew more slowly and were less angiogenic. CD31 staining showed a significant reduction in



the number of blood vessels and the size of the blood vessel lumens (Figure 6). *VEGF* expression was also reduced in the shWAVE3 tumors (Figure 6), suggesting that WAVE3 may regulate expression of VEGF and the recruit-

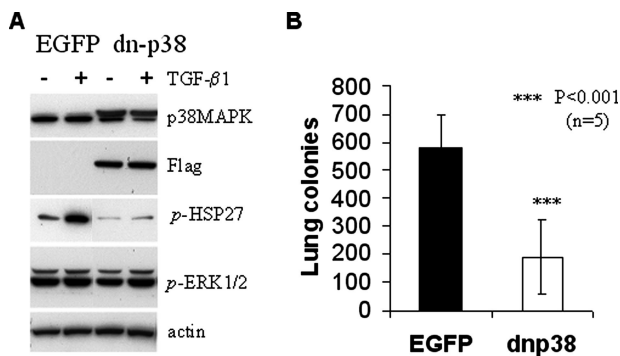
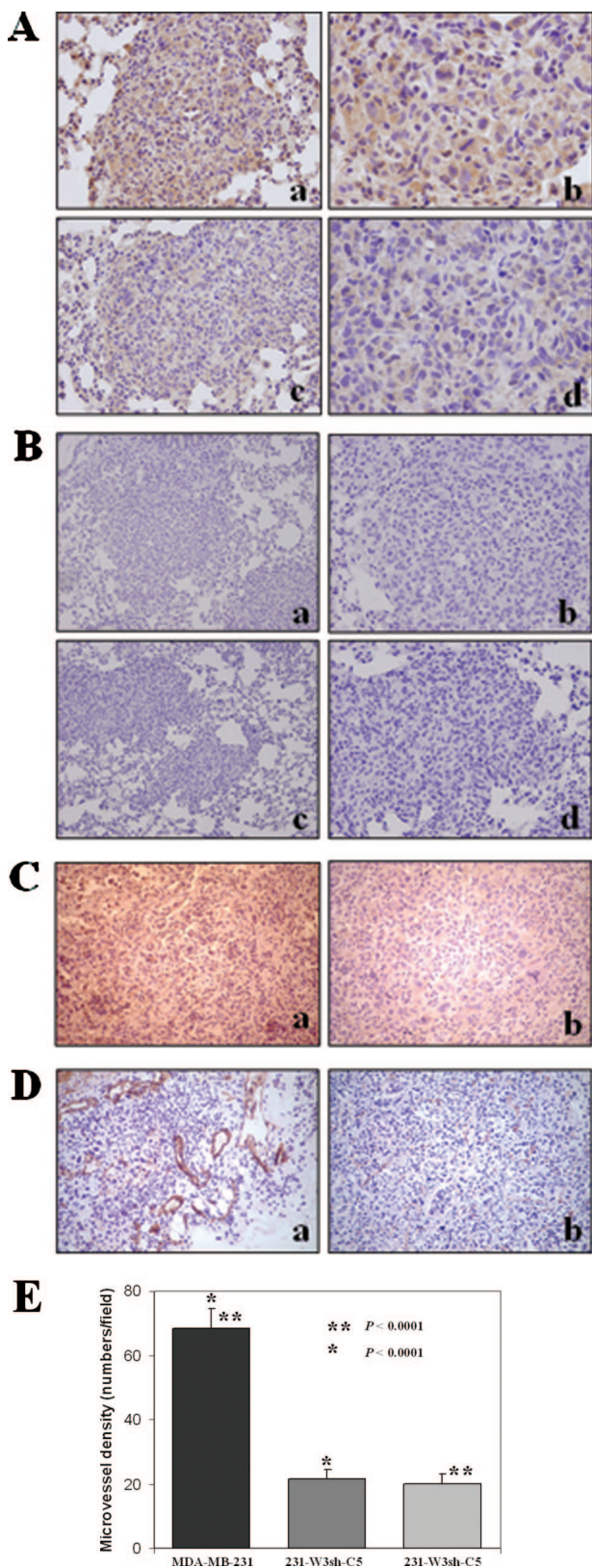


**Figure 7.** Effect of a dominant-negative p38MAPK protein on MDA-MB-231 metastasis to the lungs. **A:** Immunoblot of whole cell extracts from cells expressing either the EGFP control or FLAG-tagged dn-p38 MAPK (dn-p38). The dn-p38 protein is associated with reduced phosphorylation of HSP27 but does not affect levels of phospho-activated ERK1/2. Cells were either untreated (-), or treated (+) with 2 ng/ml TGF- $\beta$ 1 for 0 to 24 hours as indicated.  $\beta$ -Actin was used as loading control. **B:** Colonization of lung surfaces by control EGFP-transfected MDA-MB-231 cells compared with cells expressing dn-p38 cells after injection into the lateral tail vein of SCID female mice (*n*, number of mice per group).

ment of the blood vessel-forming cells. Interestingly, all three WAVE proteins are expressed in MDA-MB-231,<sup>9,10</sup> and yet, the deficiency in WAVE3 alone produced dramatic effects on tumorigenicity and the metastatic potential of tumor cells. Although this observation might suggest a unique role for WAVE3 in tumor cells, we cannot exclude the possibility that all three WAVE genes may play a role in some aspects of metastasis, given that WAVE2 also contributes to metastasis of melanoma cells.<sup>17</sup> Independent roles for the other WAVE proteins in regulating Arp2/3-mediated actin polymerization and cell migration further support this suggestion.<sup>17,21,22</sup>

There are at least two possible molecular mechanisms by which WAVE3 may contribute to tumor metastasis. Our previous studies suggest that p38MAPK is a downstream effector of WAVE3.<sup>10</sup> Here, we found that a blockade of p38MAPK signaling by dominant-negative p38MAPK (DN-p38) partially recapitulates the effect of WAVE3 on metastasis. The DN-p38 cells showed a threefold reduction in lung tumor formation compared with a sixfold reduction from cells expressing shWAVE3. As with the shWAVE3 tumors, the DN-p38 orthotopic tumors were also less angiogenic.<sup>14</sup> Given that Rac1 can activate WAVE3<sup>23</sup> as well as p38MAPK in several cell lines<sup>24,25</sup>

**Figure 6.** Immunohistochemistry analysis of the tumors derived either from the parental MDA-MB-231 cells or from the WAVE3 knockdown cells in the subcutaneous model. **A:** Staining for the WAVE3 protein in the lung tumors from wild-type MDA-MB-231 cells show high levels of WAVE3 protein (**a, b**), compared with one of the rare lung metastases from cells expressing shWAVE3 (**c, d**), which shows marked reduction in WAVE3 levels, although some immunoreactivity is still seen. **B:** IgG staining as a negative control for the WAVE3 antibody in tumors from parental MDA-MB-231 (**a, b**) and of tumors from cells expressing shWAVE3 (**c, d**). **C:** Immunostaining for VEGF shows higher immunoreactivity in the MDA-MB-231-derived tumor (**a**), compared with the tumors derived from the WAVE3 knockdown cells (**b**). **D:** Immunostaining for CD31 demonstrates relatively large numbers of blood vessels and abnormal tumor vasculature in the MDA-MB-231-derived tumors (**a**), whereas fewer and more regular-shaped blood vessels are seen in the WAVE3 knockdown-derived tumors (**b**). **E:** Microvessel density within tumor sections was determined in five fields of each tumor section, and presented as the mean number of microvessels per field. Original magnifications:  $\times 100$  (**Aa, Ac, Bb, Bd**);  $\times 400$  (**Ab, Ad, E**);  $\times 40$  (**Ba, Bc**).

including MDA-MB231,<sup>26</sup> it is suggestive that WAVE3 is required for Rac1-mediated activation of p38MAPK. It is still not clear, however, how WAVE3 affects p38MAPK activity and what the intermediate effectors are. For example, WAVE3 may be involved in Rac1-dependent activation of PAK1, an upstream kinase in the p38MAPK cascade.<sup>27</sup> Although p38MAPK may contribute to some of the WAVE3 effects, other factors such as Arp2/3 can also mediate WAVE3 effects on tumor cell motility, invasiveness, and metastasis. Cell motility is tightly regulated by the actin-filament remodeling Arp2/3 complex,<sup>11,28</sup> which is a primary target of the WASP/WAVE proteins.<sup>2,10,12</sup> Our previous studies have indicated that WAVE3 in MDA-MB-231 cells is involved in the regulation of lamellipodia production, actin stress fibers formation, and focal adhesions assembly.<sup>9</sup> Thus, WAVE3 may also contribute to anchorage-independent cell growth and cell death associated with detachment from extracellular matrix (anoikis).

In conclusion, our findings provide the first evidence for a possible role of WAVE3 in tumor progression and metastasis. WAVE3 may represent a marker of tumor progression and a potential target for anti-tumor therapy. This study provides the basis for future studies of the molecular and cellular mechanisms by which WAVE3 contributes to tumor growth, invasion, and metastasis. The success of the siRNA strategy and the potential involvement of p38MAPK in the influence of WAVE3 on metastasis provide opportunities for future therapeutic and clinical applications aimed at limiting cancer metastasis.

## References

- Hanahan D, Weinberg RA: The hallmarks of cancer. *Cell* 2000, 100:57–70
- Friedl P, Wolf K: Tumour-cell invasion and migration: diversity and escape mechanisms. *Nat Rev Cancer* 2003, 3:362–374
- Billadeau DD: Cell growth and metastasis in pancreatic cancer: is Vav the Rho'd to activation? *Int J Gastrointest Cancer* 2002, 31:5–13
- Li Y, Tondravi M, Liu J, Smith E, Haudenschild CC, Kaczmarek M, Zhan X: Cortactin potentiates bone metastasis of breast cancer cells. *Cancer Res* 2001, 61:6906–6911
- Michiels F, Habets GG, Stam JC, van der Kammen RA, Collard JG: A role for Rac in Tiam1-induced membrane ruffling and invasion. *Nature* 1995, 375:338–340
- Yoshioka K, Foletta V, Bernard O, Itoh K: A role for LIM kinase in cancer invasion. *Proc Natl Acad Sci USA* 2003, 100:7247–7252
- Lee TY, Gotlieb AI: Rho and basic fibroblast growth factor involvement in centrosome redistribution and actin microfilament remodeling during early endothelial wound repair. *J Vasc Surg* 2002, 35:1242–1252
- Suetsugu S, Takenawa T: Regulation of cortical actin networks in cell migration. *Int Rev Cytol* 2003, 229:245–286
- Sossey-Alaoui K, Li X, Ranalli TA, Cowell JK: WAVE3-mediated cell migration and lamellipodia formation are regulated downstream of phosphatidylinositol 3-kinase. *J Biol Chem* 2005, 280:21748–21755
- Sossey-Alaoui K, Ranalli TA, Li X, Bakin AV, Cowell JK: WAVE3 promotes cell motility and invasion through the regulation of MMP-1, MMP-3, and MMP-9 expression. *Exp Cell Res* 2005, 308:135–145
- Pollard TD, Borisy GG: Cellular motility driven by assembly and disassembly of actin filaments. *Cell* 2003, 112:453–465
- Takenawa T, Miki H: WASP and WAVE family proteins: key molecules for rapid rearrangement of cortical actin filaments and cell movement. *J Cell Sci* 2001, 114:1801–1809
- Sossey-Alaoui K, Su G, Malaj E, Roe B, Cowell JK: WAVE3, an actin-polymerization gene, is truncated and inactivated as a result of a constitutional t(1;13)(q21;q12) chromosome translocation in a patient with ganglioneuroblastoma. *Oncogene* 2002, 21:5967–5974
- Safina A, Vandette E, Bakin AV: ALK5 promotes tumor angiogenesis by upregulating matrix metalloproteinase-9 in tumor cells. *Oncogene* 2007, 26:2407–2422
- Cailleau R, Mackay B, Young RK, Reeves Jr WJ: Tissue culture studies on pleural effusions from breast carcinoma patients. *Cancer Res* 1974, 34:801–809
- Richert MM, Phadke PA, Matters G, DiGirolamo DJ, Washington S, Demers LM, Bond JS, Manni A, Welch DR: Metastasis of hormone-independent breast cancer to lung and bone is decreased by alpha-difluoromethylornithine treatment. *Breast Cancer Res* 2005, 7:R819–R827
- Kurusu S, Suetsugu S, Yamazaki D, Yamaguchi H, Takenawa T: Rac-WAVE2 signaling is involved in the invasive and metastatic phenotypes of murine melanoma cells. *Oncogene* 2005, 24:1309–1319
- Eden S, Rohatgi R, Podtelejnikov AV, Mann M, Kirschner MW: Mechanism of regulation of WAVE1-induced actin nucleation by Rac1 and Nck. *Nature* 2002, 418:790–793
- Gautreau A, Ho HY, Li J, Steen H, Gygi SP, Kirschner MW: Purification and architecture of the ubiquitous Wave complex. *Proc Natl Acad Sci USA* 2004, 101:4379–4383
- Innocenti M, Zucconi A, Disanza A, Frittoli E, Arecas LB, Steffen A, Stradal TE, Di Fiore PP, Carlier MF, Scita G: Abi1 is essential for the formation and activation of a WAVE2 signalling complex. *Nat Cell Biol* 2004, 6:319–327
- Suetsugu S, Yamazaki D, Kurusu S, Takenawa T: Differential roles of WAVE1 and WAVE2 in dorsal and peripheral ruffle formation for fibroblast cell migration. *Dev Cell* 2003, 5:595–609
- Yan C, Martinez-Quiles N, Eden S, Shibata T, Takeshima F, Shinkura R, Fujiwara Y, Bronson R, Snapper SB, Kirschner MW, Geha R, Rosen FS, Alt FW: WAVE2 deficiency reveals distinct roles in embryogenesis and Rac-mediated actin-based motility. *EMBO J* 2003, 22:3602–3612
- Miki H, Fukuda M, Nishida E, Takenawa T: Phosphorylation of WAVE downstream of mitogen-activated protein kinase signaling. *J Biol Chem* 1999, 274:27605–27609
- Coso OA, Chiariello M, Yu JC, Teramoto H, Crespo P, Xu N, Miki T, Gutkind JS: The small GTP-binding proteins Rac1 and Cdc42 regulate the activity of the JNK/SAPK signaling pathway. *Cell* 1995, 81:1137–1146
- Minden A, Lin A, Claret FX, Abo A, Karin M: Selective activation of the JNK signaling cascade and c-Jun transcriptional activity by the small GTPases Rac and Cdc42Hs. *Cell* 1995, 81:1147–1157
- Bakin AV, Rinehart C, Tomlinson AK, Arteaga CL: p38 mitogen-activated protein kinase is required for TGFbeta-mediated fibroblastic transdifferentiation and cell migration. *J Cell Sci* 2002, 115:3193–3206
- Zhang S, Han J, Sells MA, Chernoff J, Knaus UG, Ulevitch RJ, Bokoch GM: Rho family GTPases regulate p38 mitogen-activated protein kinase through the downstream mediator Pak1. *J Biol Chem* 1995, 270:23934–23936
- Lambrechts A, Van Troys M, Ampe C: The actin cytoskeleton in normal and pathological cell motility. *Int J Biochem Cell Biol* 2004, 36:1890–1909